Article

Cell Reports

Parallel Lineage-Tracing Studies Establish Fibroblasts as the Prevailing *In Vivo* Adipocyte Progenitor

Graphical Abstract

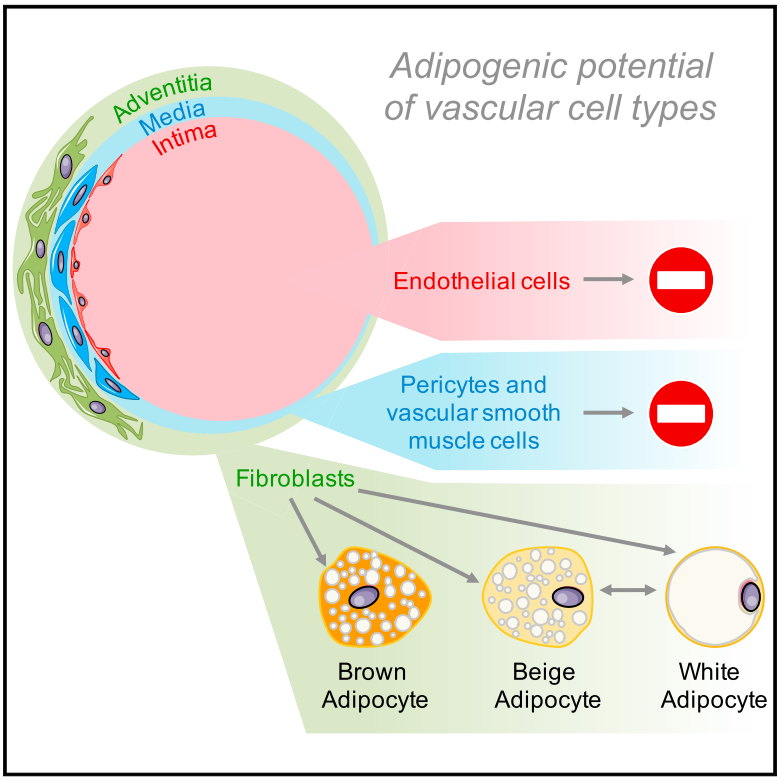

Highlights

- In adipose tissue (AT), PDGFRβ expression is not specific to mural cells
- Mural and endothelial cells have no significant adipogenic potential
- Fibroblasts have significant adipogenic potential in both white and brown AT
- Fibroblasts significantly contribute to the beiging of white AT

Authors

Paola Cattaneo, Debanjan Mukherjee, Simone Spinozzi, ..., Stefanie Dimmeler, Sylvia M. Evans, Nuno Guimarães-Camboa

Correspondence

syevans@health.ucsd.edu (S.M.E.), ncamboa@med.uni-frankfurt.de (N.G.-C.)

In Brief

Cattaneo et al. used genetic fate mapping in murine models to test the adipogenic potential of distinct cell types of the vascular wall. These parallel lineage-tracing experiments reveal that fibroblasts are the sole vascular cell type with significant adipocyte progenitor activity, giving rise to brown, beige, and white adipocytes.

Cattaneo et al., 2020, Cell Reports *30*, 571–582
January 14, 2020
https://doi.org/10.1016/j.celrep.2019.12.046

CellPress

Cell Reports
Article

Parallel Lineage-Tracing Studies Establish Fibroblasts as the Prevailing *In Vivo* Adipocyte Progenitor

Paola Cattaneo,[1,2,11] Debanjan Mukherjee,[3,4,11] Simone Spinozzi,[5] Lunfeng Zhang,[6] Veronica Larcher,[3] William B. Stallcup,[7] Hiroshi Kataoka,[8] Ju Chen,[5] Stefanie Dimmeler,[3,9] Sylvia M. Evans,[5,6,10,*] and Nuno Guimarães-Camboa[3,9,12,*]

[1]Institute of Genetic and Biomedical Research (IRGB), UOS of Milan, National Research Council of Italy, Milan 20138, Italy
[2]Humanitas Clinical and Research Center – IRCCS, Rozzano (MI) 20089, Italy
[3]Institute of Cardiovascular Regeneration, Goethe University, Frankfurt 60590, Germany
[4]International Max Planck Research School for Heart and Lung Research, Bad Nauheim 61231, Germany
[5]Department of Medicine, University of California at San Diego, La Jolla, CA 92093, USA
[6]Skaggs School of Pharmacy, University of California at San Diego, La Jolla, CA 92093, USA
[7]Tumor Microenvironment and Cancer Immunology Program, Cancer Center, Sanford Burnham Prebys Medical Discovery Institute, La Jolla, CA 92037, USA
[8]Hirakata-Kohsai Hospital, 1-2-1 Fujisaka-Higashi-machi, Hirakata, Osaka 573-0153, Japan
[9]German Center for Cardiovascular Research, Berlin (partner site Frankfurt Rhine-Main), Germany
[10]Department of Pharmacology, University of California at San Diego, La Jolla, CA 92093, USA
[11]These authors contributed equally
[12]Lead Contact
*Correspondence: syevans@health.ucsd.edu (S.M.E.), ncamboa@med.uni-frankfurt.de (N.G.-C.)
https://doi.org/10.1016/j.celrep.2019.12.046

SUMMARY

Despite decades of studies suggesting that the *in vivo* adipocyte progenitor resides within the vascular niche, the exact nature of this progenitor remains controversial because distinct studies have attributed adipogenic properties to multiple vascular cell types. Using Cre recombinases labeling distinct vascular lineages, we conduct parallel lineage tracing experiments to assess their degree of contribution to *de novo* adipogenesis. Although we detect occasional adipocytes that were lineage traced by endothelial or mural recombinases, these are rare events. On the other hand, platelet-derived growth factor receptor alpha (PDGFRα)-expressing adventitial or capsular fibroblasts make a significant contribution to adipocytes in all depots and experimental settings tested. Our data also suggest that fibroblasts transition to an intermediate beige adipocyte phenotype prior to differentiating to a mature white adipocyte. These observations, together with histological analyses revealing that adipose tissue fibroblasts express the mural cell marker PDGFRβ, harmonize a highly controversial field with implications for multiple human diseases, including the pandemic of obesity.

INTRODUCTION

Owing to their ability to store and metabolize lipids, adipocytes are key intermediaries in physiological processes that regulate the body's energy reserves (Gesta et al., 2007; Lee et al., 2014; Rutkowski et al., 2015). Mammals have two major types of adipocytes that exhibit distinct function and cellular architecture: white adipocytes (Was) and brown adipocytes (BAs) (Gesta et al., 2007; Lee et al., 2014; Rutkowski et al., 2015). White adipocytes are optimized for energy storage, containing a single large lipid vesicle occupying most of the cellular volume (unilocular adipocytes). This predominant lipid vesicle pushes the nucleus and a mitochondria-poor cytoplasm to a peripheral position (Gesta et al., 2007; Lee et al., 2014; Rutkowski et al., 2015). On the other hand, brown adipocytes have smaller dimensions, contain numerous lipid droplets of small diameter (multilocular adipocytes), and are equipped with specialized mitochondria that burn lipids to produce heat (non-shivering thermogenesis) (Gesta et al., 2007; Lee et al., 2014; Rutkowski et al., 2015). More recently, a third type of adipocytes has been proposed: beige adipocytes (bAs) (Wu et al., 2012). These have a multilocular structure apparently identical to that of brown adipocytes; however, rather than being found in brown adipose tissue (BAT), beige adipocytes are found in white adipose tissue (WAT), nestled between white adipocytes. The relative abundance of beige adipocytes in WAT can be increased by exposure to cold (Barbatelli et al., 2010; Young et al., 1984) or stimulation with β3-adrenergic receptor agonists (Granneman et al., 2005; Himms-Hagen et al., 2000; Nagase et al., 1996) in a process referred to as beiging of white fat.

Adipose depots are highly plastic tissues. When caloric consumption exceeds metabolic demands, white adipose depots enlarge to store energy surplus in the form of triglycerides. When caloric intake is insufficient to satisfy metabolic demands, white adipose depots shrink, releasing energy in the form of fatty acids (Gesta et al., 2007; Lee et al., 2014; Rutkowski et al., 2015). Expansion of adipose depots takes place through two distinct mechanisms: production of new adipocytes from adipocyte

progenitors (APs) (*de novo* adipogenesis) and enlargement of preexisting adipocytes (adipocyte hypertrophy) (Gesta et al., 2007; Lee et al., 2014; Rutkowski et al., 2015). The relative contribution of these two processes to the growth of adipose depots is variable and dependent on diverse factors, including age, gender, diet, and nature of the depot. Rates of *de novo* adipogenesis have been estimated using two distinct recombinases expressed under the control of the adipocyte-specific adiponectin promoter, allowing time-controlled labeling of mature adipocytes: the AdipoChaser (doxycycline inducible) and adiponectin-CreER (tamoxifen inducible) (Jeffery et al., 2015; Wang et al., 2013). To get further insight into mechanisms of *de novo* adipogenesis, it would be ideal to complement these data with the inverse analysis, assessing rates of *de novo* adipogenesis using a mouse allele that labels all APs rather than the mature adipocyte. However, this task has as a prerequisite the clear identification of the *in vivo* AP.

Pioneering work by Clark and Clark almost eight decades ago revealed that *de novo* adipogenesis typically takes place in the vicinity of blood vessels, suggesting the AP as a cell type of the vascular wall (Clark and Clark, 1940). The wall of blood vessels is composed of at least three major cell types organized in concentric layers: endothelium (tunica intima), mural cells of the tunica media (pericytes in capillaries or vascular smooth muscle in larger vessels), and adventitial fibroblasts (tunica adventitia). Recent years have been marked by efforts to identify which of these cell types corresponds to the AP. Lineage-tracing studies employing constitutive or inducible Cres have attributed adipogenic potential to all three major cell types of the vascular wall: endothelial cells (Tran et al., 2012), mural cells (Tang et al., 2008; Vishvanath et al., 2016), and fibroblasts (Lee et al., 2012). Bone marrow transplant and lineage-tracing studies have also implicated hematopoietic lineages as APs (Crossno et al., 2006; Majka et al., 2010; Sera et al., 2009). However, data from distinct labs have challenged a potential contribution from endothelial and hematopoietic lineages (Berry and Rodeheffer, 2013; Koh et al., 2007), and our own work has questioned a potential contribution from mural cells (Guimaraes-Camboa et al., 2017). Conclusions from these reports, including the identity of APs and reported rates of *de novo* adipogenesis, are often seemingly contradictory and, due to this, the exact nature of APs has remained elusive. Metanalysis of published literature is also a highly challenging task, as these lineage-tracing studies were performed in different laboratories, often using diverse experimental conditions and typically focusing on a single cell type rather than testing distinct cell lineages side by side.

Here, we conducted parallel lineage-tracing studies using Cre recombinases that separately label the three major cell types within the vascular wall (endothelium, mural cells, and fibroblasts). In our search for suitable recombinase drivers, we observed that platelet-derived growth factor receptor beta (PDGFRβ), frequently used as a mural cell marker, is not mural cell specific within adipose depots, as it is also robustly expressed by fibroblasts. On the other hand, our *Tbx18-CreERT2* allele is highly restricted to mural cells, allowing tracking of the progeny of mural cells in multiple experimental settings. Importantly, we found that a *Pdgfra-MerCreMer* allele previously generated to study PDGFRα-expressing populations during embryogenesis (Ding et al., 2013) was an ideal tool to selectively label adipose tissue fibroblasts *in vivo*. Using these two alleles and *Tie2-Cre* (Kisanuki et al., 2001) (labeling endothelial and hematopoietic lineages), we conducted lineage-tracing studies in adult male mice fed chow or a lard-based high-fat diet (HFD), with 60% of kilocalories from fat (Vishvanath et al., 2017). Our results clearly revealed that fibroblasts are the only cells of the vascular wall with significant adipogenic potential *in vivo* in both WAT and BAT. Importantly, our studies in male mice showed that despite inducing a significant increase in body weight, HFD resulted in increased *de novo* adipogenesis from fibroblast progenitors only in perigonadal WAT (pgWAT). In inguinal WAT (ingWAT) and interscapular BAT (iBAT), HFD did not significantly alter the percentage of *Pdgfra-MerCreMer*-derived adipocytes, consistent with previous results showing depot-specific responses to high caloric intake in males (Jeffery et al., 2015; Wang et al., 2013). Our histological analyses also suggested that in pgWAT, in addition to perivascular fibroblasts, fibroblasts of the mesenchymal layers encapsulating the tissue were also capable of adipogenic differentiation. Finally, observation of early time points during pulse-chase experiments suggested that in white adipose depots, fibroblast progenitors follow a gradual differentiation cascade, initially acquiring a beige phenotype prior to differentiating into a fully mature white adipocyte. Beiging experiments stimulated by a β3-adrenergic agonist revealed a significant contribution from fibroblastic progenitors, without significant contribution from any other vascular cell type, including vascular smooth muscle (labeled by *Myh11-CreERT2* and *Tbx18Cre-ERT2*).

RESULTS

Selective Labeling of Major Vascular Cell Types

Cells comprising the three tunicae of the vascular wall can be easily identified in large vessels, such as the aortic artery (Figures 1A and 1B). In vessels of small diameter, the three tunica are less evident, and their visualization requires immunostaining with lineage-specific antibodies (Figures 1C and 1D). Endothelial cells can easily be identified by a wide variety of specific markers such as - CD31/PECAM1 (Platelet Endothelial Cell Adhesion Molecule 1), or ERG (ETS-Related Gene) - and adventitial fibroblasts can be labeled using the pan-fibroblast marker PDGFRα, Figures 1A–1D) (Andrae et al., 2008). Strategies for identification of mural cells are dependent on vessel caliber: vascular smooth muscle cells surrounding large- and medium-sized vessels can be detected by expression of contractile proteins (ACTA2/αSMA or MYH11/smMHC; Figures 1A–1D), but there are few markers that selectively mark pericytes surrounding smaller vessels. A frequent strategy to distinguish pericytes resides on immunostaining for PDGFRβ (Armulik et al., 2011). However, our histological analyses revealed that PDGFRβ is not restricted to mural cells and is also widely expressed by PDGFRα$^+$ adventitial fibroblasts of the aorta and vessels within adipose depots (Figures 1E–1H and S1). As such, in adipose depots, a transgenic inducible Cre expressed under the control of a large fragment of the *Pdgfrb* promoter (Vishvanath et al., 2016) would be expected to label both mural cells and adventitial fibroblasts. Importantly, we have previously established active expression of the

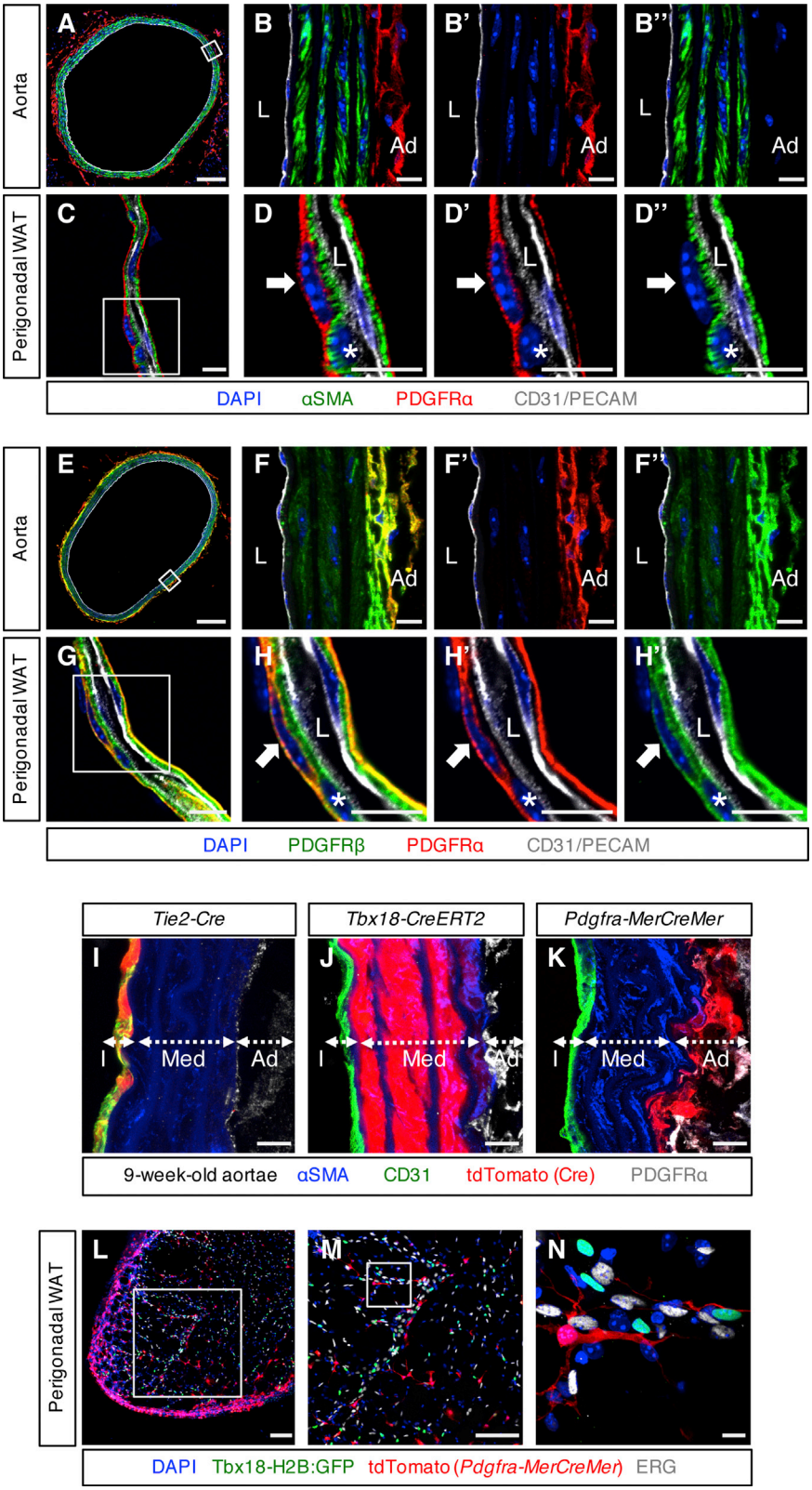

Figure 1. Strategies for Identifying and Lineage Tracing Distinct Cell Types of the Vascular Wall

(A–D) immunostaining with antibodies against the endothelial cell antigen CD31/PECAM1, smooth muscle actin (αSMA), and the fibroblast marker PDGFRα allowed visualization of distinct vascular cell types in large vessels such as the aorta (A and B), as well as smaller vessels within adipose depots (C and D).

(E–H) Co-immunostaining for both PDGFRs (α and β) revealed that in addition to mural cells (vascular smooth muscle and pericytes), PDGFRβ (green) is also strongly expressed by adventitial fibroblasts of the aorta (E and F) and of blood vessels located within perigonadal adipose tissue (G and H).

(B), (D), (F), and (H) represent higher magnifications of areas boxed in (A), (C), (E), and (G), respectively.

(I–K) Lineage tracing with distinct Cre alleles allowed labeling of specific cell types within the vascular wall. *Tie2-Cre* labeled all endothelial cells of the intima (I), *Tbx18-CreERT2* efficiently labeled vascular support cells of the media (J), and *Pdgfra-MerCreMer* efficiently labeled adventitial fibroblasts (K).

(L–N) Within perigonadal adipose tissue, in addition to efficiently labeling adventitial fibroblasts in vessels of distinct calibers, *Pdgfra-MerCreMer* also labeled fibroblasts of the mesenchymal capsule surrounding the tissue. (L) Low magnification of a *Pdgfra-MerCreMer/WT; Tbx18-H2B:GFP/WT; Rosa26-tdTomato/WT* perigonadal adipose depot revealing the overall pattern of labelling by *Pdgfra-MerCreMer*. (M and N) Higher magnification panels of boxed areas show that lineage-traced fibroblasts (red), endothelial cells (ERG+, gray) and mural cells (Tbx18-H2B:GFP+, green) were mutually exclusive events.

Ad, adventitia; I, intima; L, lumen; M, media. Bars represent 100 μm in (A), (E), (L), and (M) and 10 μm in all other panels.

See also Figure S1.

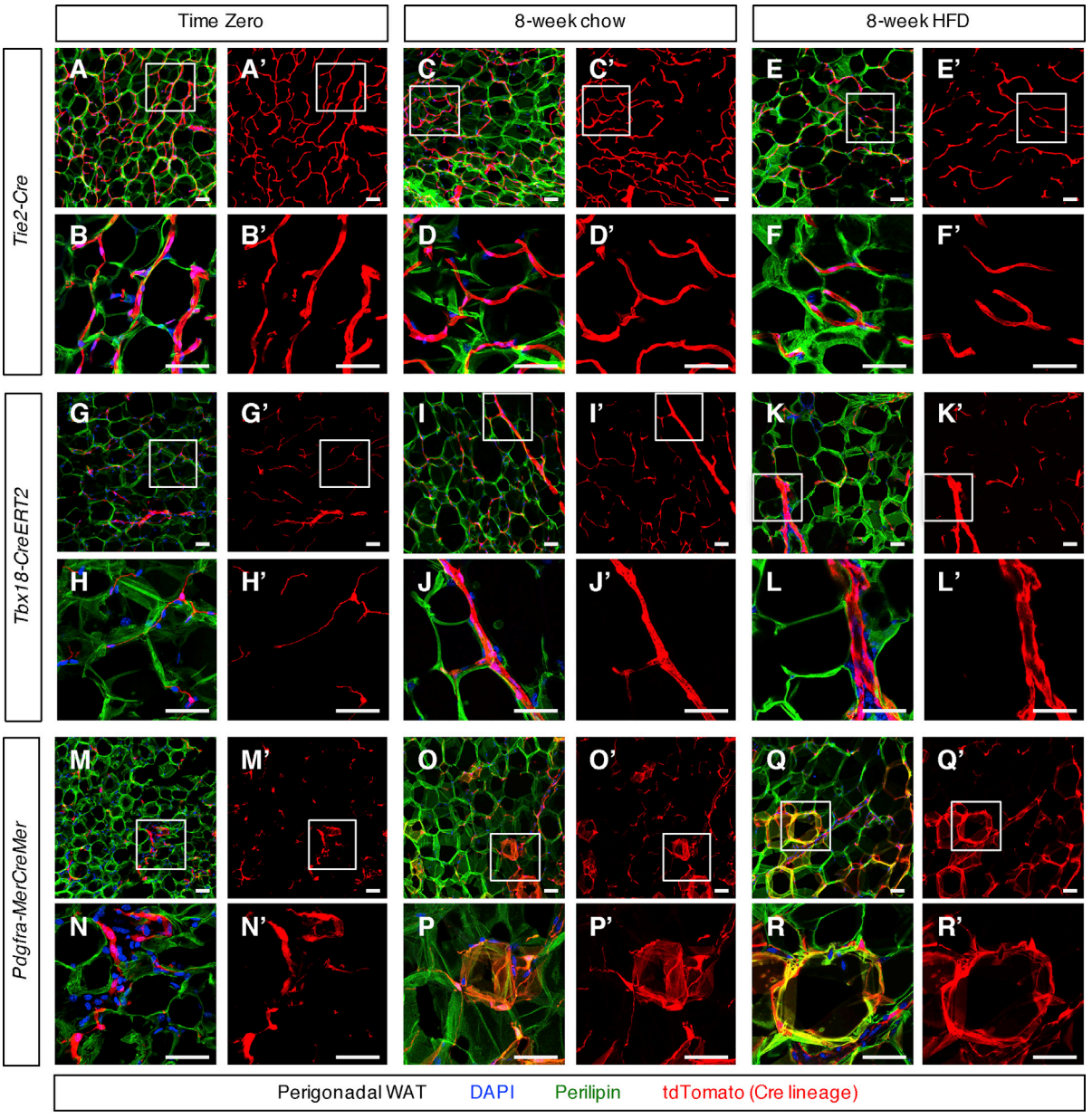

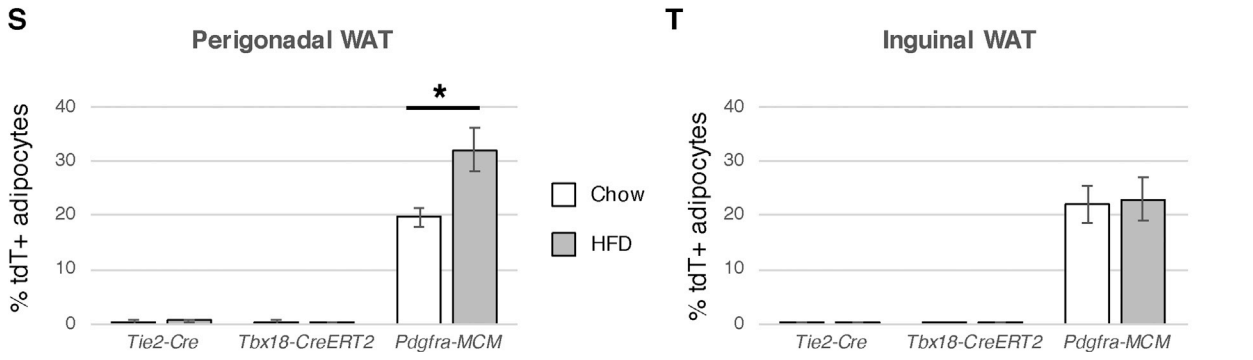

(legend on next page)

transcription factor *Tbx18* as a robust strategy for specific identification of mural cells (pericytes and vascular smooth muscle cells) in adipose depots (Guimaraes-Camboa et al., 2017).

For lineage-tracing purposes, permanent genetic labeling of vascular cell lineages can be achieved by combining the red fluorescent *Rosa26-tdTomato* reporter allele (Madisen et al., 2010) with distinct Cre drivers. Endothelial and hematopoietic lineages are efficiently labeled by a widely used *Tie2-Cre* allele (Kisanuki et al., 2001) (Figure 1I), and labeling of mural cells (both pericytes and vascular smooth muscle) can be achieved using a *Tbx18-CreERT2* allele that we have previously characterized (Guimaraes-Camboa et al., 2017) (Figure 1J). To promote selective labeling of fibroblasts, we tested a *Pdgfra-MerCreMer* previously generated for the study of PDGFRα^+ populations in mouse embryogenesis (Ding et al., 2013). Upon tamoxifen administration, *Pdgfra-MerCreMer/WT; Rosa26-tdTomato/WT* animals displayed robust labeling of adventitial fibroblasts in the aorta (Figure 1K). Analyses of perigonadal and inguinal fat depots revealed two major domains of labeling: adventitial fibroblasts located in the vicinity of large and small blood vessels within the tissue, and fibroblasts within the mesenchymal capsule that externally delimits these adipose depots (Figures 1L–1N and S1). Validating the *Pdgfra-MerCreMer* as a tool to selectively label adventitial and capsular fibroblasts without hitting other populations of vascular cells, histological analyses revealed that cells labeled by this Cre did not express the endothelial cell marker ERG or the mural cell marker *Tbx18-H2B:GFP* (Figures 1L–1N).

Lineage Tracing Reveals Fibroblasts as the Sole Vascular Cell Type Contributing to *De Novo* Adipogenesis

Having established genetic strategies to permanently label the three major cell types of the vascular wall, we conducted parallel lineage-tracing studies using the *Rosa26-tdTomato* lineage indicator (Madisen et al., 2010) to assess which of these lineages had the potential to significantly contribute to *de novo* adipogenesis. To this end, animals were induced (except for the constitutive *Tie2-Cre* line) with daily intraperitoneal injections of tamoxifen for three consecutive days, starting at 8 weeks of age. For each Cre allele, a minimum of three animals were euthanized 1 day after conclusion of the tamoxifen pulse for assessment of time-zero labeling patterns. The remaining animals were allowed a chase of 8 weeks prior to harvesting tissues for histological analyses. To evaluate the relevance of caloric intake on the rate of *de novo* adipogenesis from distinct vascular cell types, during the chase period, mice were divided into two distinct experimental groups: 8-week chow (Teklad LM-485, Envigo) and 8-week HFD (60% of kilocalories from fat, Research diets Inc., D12492). At the end of the experimental term, animals fed chow had gained 22% of their initial weight assessed at time zero, whereas animals fed HFD gained 57% of their initial weight assessed at time zero (Figure S2A). Recent reports have suggested that tamoxifen can promote weight loss (13% weight loss 6 days post administration) due to adipocyte death, a process followed by a compensatory wave of *de novo* adipogenesis (Ye et al., 2015). We did not observe this effect, as animals of both experimental groups (chow and HFD) displayed increased body weight 1 week post-tamoxifen induction (8.7% increase in the chow group and 6.2% in HFD; Figure S2A). To produce a dataset representative of distinct types of adipose tissue, we analyzed three major adipose depots: pgWAT (a type of coelomic WAT), ingWAT (a type of subcutaneous WAT), and iBAT (the major brown adipose depot in the mouse body). For quantification of rates of adipocyte labeling by tdTomato, all tissues were sectioned and immunostained with the adipocyte marker perilipin (Blanchette-Mackie et al., 1995), allowing easy identification of individual unilocular white adipocytes. For each genotype and condition, we analyzed a minimum of three animals and five histological sections per animal (per animal, on average, we imaged and quantified 719 adipocytes in pgWAT and 1,733 adipocytes in iWAT). Importantly, our analyses revealed that in both white adipose depots analyzed, fibroblasts labeled by *Pdgfra-MerCreMer* were the only vascular cell type significantly contributing to *de novo* adipogenesis (Figures 2 and S2). Rare examples of white adipocyte labeling by *Tie2-Cre* and *Tbx18Cre-ERT2* could be found both in perigonadal and ingWAT, but at extremely low rates (*Tbx18CreERT2* 8-week chow labeling = 0.04% in iWAT and 0.43% in pgWAT; *Tie2-Cre* 8-week chow labeling = 0.25% in iWAT and 0.24% in pgWAT). Comparable low labeling rates with these Cres were also observed in adipose depots from mice fed HFD, arguing against a significant contribution of either endothelial or mural cells to *de novo* adipogenesis (Figures 2S and 2T). In contrast to results with *Tie2-Cre* and *Tbx18Cre-ERT2*, 8 weeks after tamoxifen induction, *Pdgfra-MerCreMer;Rosa26-tdTomato* mice on a chow diet showed ~20% of white adipocytes labeled by tdTomato both in pgWAT and ingWAT (Figures 2O–2T, S2P, and S2Q). Since the *Pdgfra-MerCreMer* did not label white adipocytes at time zero (Figures 2M, 2N, S2N, and S2O), this observation suggested lineage-traced white adipocytes had derived from fibroblastic progenitors via *de novo* adipogenesis. In keeping with previous studies demonstrating increased *de novo* adipogenesis in response to HFD within perigonadal fat, but not

Figure 2. PDGFRα^+ Fibroblasts Were the Only Vascular Cell Type Significantly Contributing to *De Novo* Adipogenesis in WAT

(A–F) *Tie2-Cre*-labeled endothelial cells (A and B) did not acquire a white adipocyte fate in mice fed chow (C and D) or HFD (E and F).

(G–L) *Tbx18-CreERT2* labeled mural cells (G and H) did not acquire a white adipocyte fate in mice fed chow (I and J) or HFD (K and L).

(M and N) At time zero (1 day post-tamoxifen), *Pdgfra-MerCreMer* efficiently labeled fibroblasts in pgWAT.

(O–R) 8 weeks post-tamoxifen induction, *Pdgfra-MerCreMer* lineage-traced adipocytes could be found both in animals fed chow (O and P) and HFD (Q and R), indicating these cells were derived from PDGFRα-expressing progenitors by *de novo* adipogenesis.

(S and T) Quantification of rates of *de novo* adipogenesis from distinct vascular cell lineages in two major white adipose depots, pgWAT (S) and ingWAT (T), after 8 weeks of chow or HFD. Data are represented as mean ± SEM, *$p \leq 0.05$ (n = 3 per experimental group).

(B), (D), (F), (H), (J), (L), (N), (P), and (R) represent higher magnifications of areas boxed in (A), (C), (E), (G), (I), (K), (M), (O), and (Q), respectively. Bars represent 50 μm in all panels.

See also Figures S2 and S3.

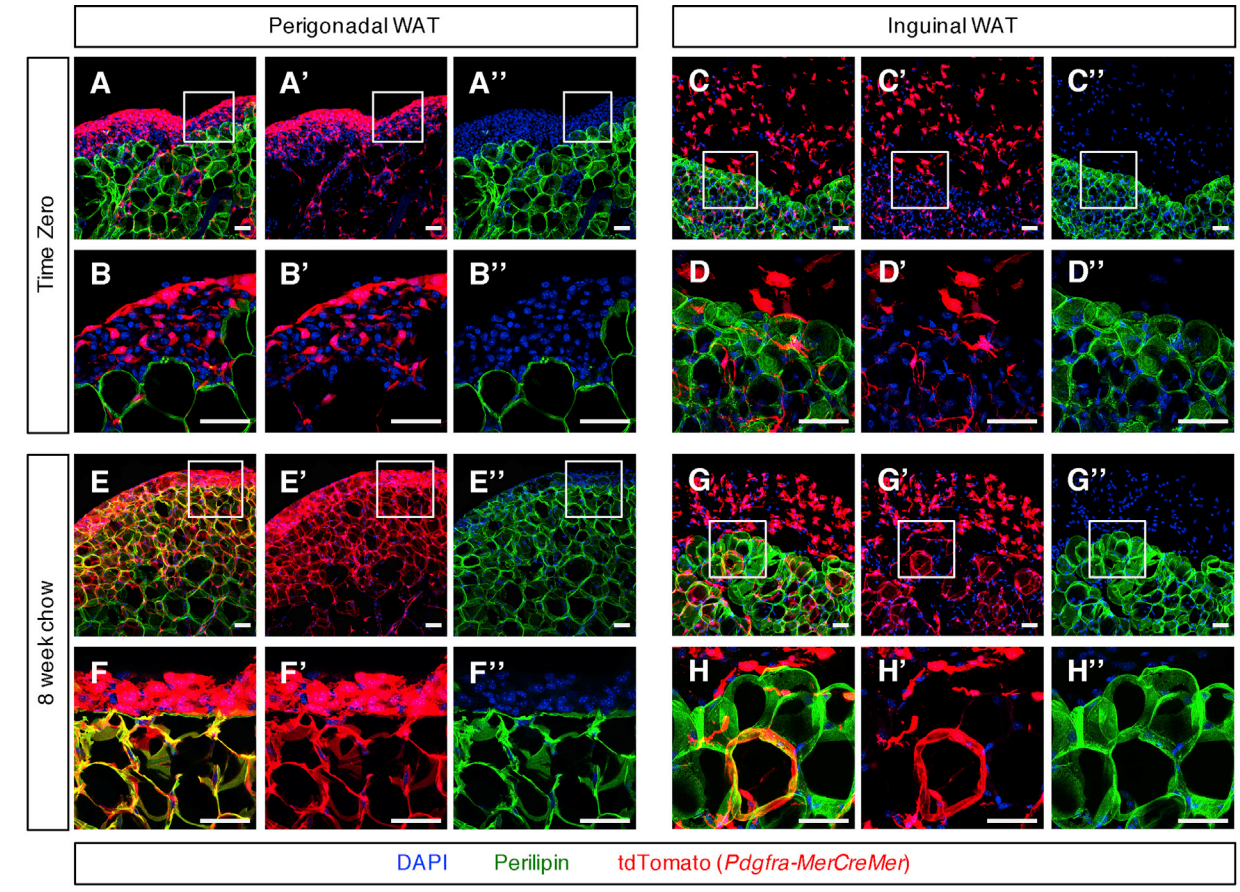

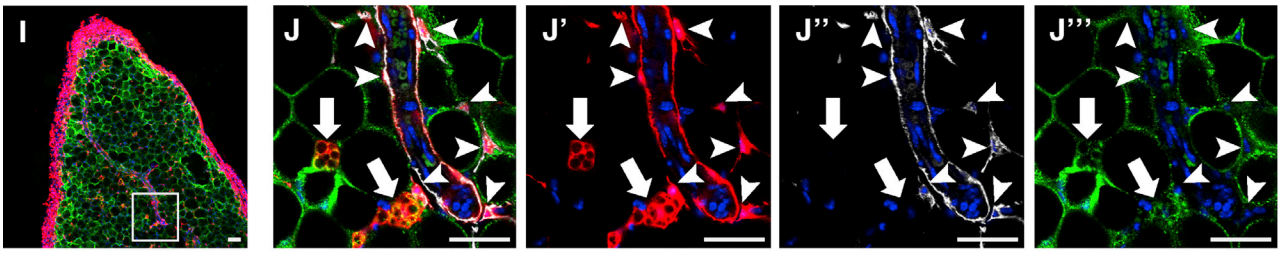

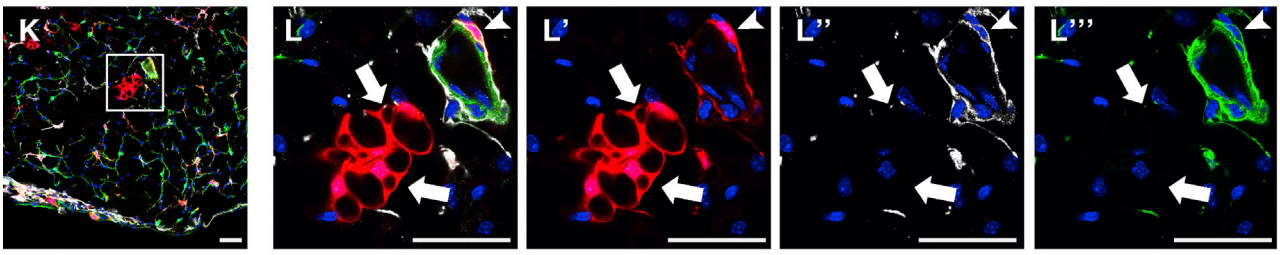

(legend on next page)

inguinal fat in males (Jeffery et al., 2015; Wang et al., 2013), HFD resulted in a further increase of labeled adipocytes in pgWAT of *Pdgfra-MerCreMer;Rosa26-tdTomato* mice (32.18% adipocyte labeling in HFD versus 19.75% in chow), but not in ingWAT (23.02% adipocyte labeling in HFD versus 22.25% in chow; Figures 2S and 2T). Notably, PDGFRα$^+$ APs were also found to differentiate to brown adipocytes within interscapular brown adipose depots (Figure S3). Importantly, the rates of *de novo* adipogenesis from PDGFRα$^+$ APs (8% adipocyte labeling after 8-week chase) in iBAT were lower than those observed in pgWAT or ingWAT and did not significantly change in animals fed HFD (Figure S3T). Altogether, these observations revealed that endothelial and mural cells do not function as APs *in vivo* and that PDGFRα$^+$ APs are the sole vascular wall cell type that significantly contributes to *de novo* adipogenesis in either WAT or BAT.

Adipogenic Potential of Capsular Fibroblasts

White adipose depots are externally surrounded by a capsule of fibroblasts that also get strongly labeled by the *Pdgfra-MerCreMer* allele (Figure 1L). Interestingly, histological examination revealed this external mesenchymal lining exhibited distinct properties depending on the white adipose depot considered. In pgWAT, the mesenchymal lining (of mesothelial origin) exhibited a high cellular density, with multiple layers of fibroblasts being tightly compacted in a reduced volume (Figures 3A and 3B). On the other hand, the mesenchymal capsule of ingWAT exhibited reduced cellular density and was richer in extracellular matrix (Figures 3C and 3D). Given the extremely efficient labeling of capsular fibroblasts at time zero (Figures 3A–3D), we looked for evidence of *de novo* adipogenesis from these cells. Interestingly, in pgWAT, 8 weeks post-tamoxifen, we could observe areas in which the vast majority of adipocytes in the vicinity of the mesenchymal capsule were lineage traced by *Pdgfra-MerCreMer*, strongly suggesting these adipocytes were derived from capsular serosal mesothelial fibroblasts (Figures 3E and 3F). Importantly, these areas of high-density labeling were found sporadically rather than being present throughout the tissue, suggesting that the adipogenic progenitor potential was restricted to a subset of capsular fibroblasts or that subsets of progenitors were being sporadically activated. Moreover, areas of high-density labeling of sub-mesothelial adipocytes could be found in pgWAT of animals fed chow or HFD but were absent from inguinal white adipose depots (Figures 3G and 3H), indicating that depot-intrinsic properties, rather than caloric intake, condition the progenitor potential of capsular fibroblasts.

De Novo White Adipogenesis Involves a Beige Phenotype Intermediate

Having observed evidence for significant *de novo* adipogenesis from fibroblast progenitors, we sought to understand the dynamics of the process allowing the conversion of a fibroblast to a fat-storing cell. As revealed in Figures 1, 2, and S2, at time zero, *Pdgfra-MerCreMer* efficiently labeled fibroblasts without labeling white adipocytes. However, when we analyzed samples harvested at very early phases of the chase period (5 days post-tamoxifen), lineage-traced fibroblasts started adopting a beige adipocyte phenotype (small dimensions and multiple lipid droplets) nestled between fully differentiated white adipocytes (arrows in Figures 3I and 3J). Focusing on cells lineage traced by *Pdgfra-MerCreMer*, these early adipocytes had already completely lost cell-surface markers of their fibroblast progenitors: PDGFRα and PDGFRβ (Figures 3I–3L). After 8 weeks of chow or HFD, all lineage-traced adipocytes had adopted a unilocular white adipocyte phenotype (Figures 2 and S2), suggesting progressive differentiation from fibroblast to intermediate beige adipocyte before adoption of the white adipocyte phenotype.

Fibroblastic APs Contribute to Beiging of WAT

The frequency of beige adipocytes found within white depots can be dramatically increased by stimuli such as exposure to cold or adrenergic stimulation (beiging of WAT) (Giordano et al., 2016; Lee et al., 2014). Cellular mechanisms leading to WAT beiging remain controversial; experiments with the Adipo-Chaser mouse indicated that beiging takes place mainly by *de novo* adipogenesis from APs (Wang et al., 2013), but distinct reports have suggested that beiging takes place by transdifferentiation of white adipocytes into beige adipocytes (Barbatelli et al., 2010; Himms-Hagen et al., 2000). As for *de novo* white adipogenesis, distinct populations of APs have been proposed as contributors to *de novo* beige adipogenesis, including smooth muscle cells (Long et al., 2014) or PDGFRα$^+$ cells (Lee et al., 2012). Considering the controversy in the literature and given the physiological importance of beiging of white fat (Giordano et al., 2016), we decided to test the progenitor potential of the three major vascular cell types in a setting of WAT beiging. To

Figure 3. Spatiotemporal Dynamics of *De Novo* Adipogenesis from PDGFRα-Expressing Progenitors

(A–D) *Pdgfra-MerCreMer* efficiently labeled fibroblasts of the mesenchymal capsules externally surrounding pgWAT (A and B) and ingWAT (C and D). The overall architecture and cellular density of this external capsule was significantly different between both depots. (B) and (D) represent higher magnifications of areas boxed in (A) and (C), respectively.

(E and F) In pgWAT, 8 weeks post-tamoxifen, examples of extremely abundant adipocyte labeling by *Pdgfra-MerCreMer* could be found in the vicinity of the external mesenchymal capsule, independently of the dietary regimen employed.

(G and H) These areas of extensive adipocyte labeling in the pericapsular region were not observed in ingWAT.

(F) and (H) represent higher magnifications of areas boxed in (E) and (G), respectively.

(I–L) Images of *Pdgfra-MerCreMer* lineage-traced perigonadal and ingWAT 5 days post-tamoxifen showing early stages of adipogenesis from fibroblastic progenitors. (J) and (L) represent higher magnifications of areas boxed in (I) and (K), respectively.

(I and J) In the early stages of differentiation, *Pdgfra-MerCreMer* lineage-traced adipocytes exhibited a beige adipocyte phenotype of small cells with multiple lipid vesicles that were nestled between mature unilocular white adipocytes. These early adipocytes (arrows) were positive for the adipocyte marker perilipin (green), but, despite being lineage traced by *Pdgfra-MerCreMer*, did not express PDGFRα protein (gray), distinguishing them from adjacent PDGFRα$^+$ fibroblasts (arrowheads).

(K and L) In addition to losing PDGFRα protein (gray), differentiating adipocytes (arrows) had also lost expression of PDGFRβ (green). Bars represent 50 μm in all panels.

this end, we conducted lineage-tracing analyses in mice exposed to a low dose (osmotic minipump release of 0.75 nmol/h for 14 consecutive days prior to euthanasia) of CL316,243 (CL), a β3-adrenergic receptor agonist that induces beiging of white depots without signs of lipolysis-induced inflammation (Granneman et al., 2005; Lee et al., 2012). Previous studies proposing a smooth muscle origin for beige adipocytes (Long et al., 2014) were based on lineage tracing approaches using a transgenic allele expressing an inducible Cre under the control of the smooth muscle myosin heavy chain promoter (*Myh11-CreERT2* or smMHC-*CreERT2*) (Wirth et al., 2008). Thus, in addition to the three Cre alleles used for lineage-tracing experiments for *de novo* adipogenesis in WAT and BAT, we also utilized the same *Myh11-CreERT2* used by Long et al. (2014) in our experiments to address beiging of WAT. Characterization of time-zero labeling patterns of pgWAT and ingWAT depots from *Myh11-CreERT2;Rosa26-tdTomato* mice revealed that in addition to vascular smooth muscle cells, *Myh11-CreERT2* also labeled multiple perivascular cells that did not express proteins of the mature vascular smooth muscle contractile apparatus but were positive for PDGFRβ (Figure S4A). Expression of PDGFRβ placed these non-smooth-muscle lineage-traced cells as either fibroblasts or pericytes. To address the nature of such cells, we analyzed the adipose depots of mice that were lineage traced by *Myh11-CreERT2* and had a copy of the *Tbx18-H2B:GFP* allele, marking mural cells. These analyses revealed a complete overlap between tdTomato and GFP fluorescent signals, indicating *Myh11-CreERT2* labels both mature vascular smooth muscle and pericyte in a pattern that closely resembles the one produced by *Tbx18-CreERT2* (Figures S4B–S4D). Analyses of ingWAT of mice 14 days following CL treatment revealed no evidence for significant conversion of pericytes or vascular smooth muscle cells to beige adipocytes using *Myh11-CreERT2 or Tbx18-CreERT2* (Figures 4C–4F), a finding consistent with recent reports (Jiang et al., 2017). Similarly, utilizing *Tie2-Cre*, we also found no evidence for a significant contribution of endothelial or hematopoietic cells to *de novo* beiging of WAT, although rare labeled adipocytes were observed (Figures 4A and 4B). On the other hand, *Pdgfra-MerCreMer* labeled a high number of multilocular beige adipocytes, frequently found in clusters of adjacent cells (Figures 4G and 4H). Importantly, even though *Pdgfra-MerCreMer* labeled ~19% of all beige adipocytes in ingWAT, the majority (81%) of multilocular cells observed after CL treatment were not lineage traced (Figure 4I), in agreement with the idea that, despite the significant contribution from APs, a white-to-beige phenotypic switch from preexisting white adipocytes is the major contributor to beiging in ingWAT (Barbatelli et al., 2010; Himms-Hagen et al., 2000; Jiang et al., 2017).

DISCUSSION

To clarify ongoing controversies as to the identity of the *in vivo* AP, we have conducted parallel lineage-tracing studies employing Cre alleles selectively labeling each of the vascular wall cell types. Our analyses provided quantitative assessment of the contribution of each cell type to *de novo* adipogenesis in distinct types of fat depots and harmonized seemingly contradictory results from existing literature. Importantly, parallel lineage-tracing experiments revealed that PDGFRα$^+$ fibroblasts were the sole cell type of the vascular wall with significant adipogenic potential in tamoxifen-treated animals fed either chow or HFD. Although we cannot exclude that, on rare occasions, endothelial or hematopoietic cells (*Tie2-Cre*) and mural cells (*Tbx18-CreERT2*) might contribute to *de novo* adipogenesis, extremely reduced rates of adipocyte labeling when using Cres specific to these cell types argue against a significant role for these cell types as APs, validating previous work from our groups and others (Berry and Rodeheffer, 2013; Guimaraes-Camboa et al., 2017; Koh et al., 2007). Notably, endothelial cells were particularly abundant in all adipose depots analyzed (Figures 2, S2, and S3) and often completely engulfed adipocytes. We speculate that this distribution, coupled to the reduced cytoplasmic volume of white adipocytes, might lead to mistakenly identifying adipocytes as being labeled by endothelial Cres (Berry and Rodeheffer, 2013), which might partly account for previously reported adipocyte labeling by endothelial Cres (Tran et al., 2012). We had previously shown that mural cells (pericytes and vascular smooth muscle) do not significantly contribute to *de novo* adipogenesis *in vivo* (Guimaraes-Camboa et al., 2017). However, such observations were questioned by Vishvanath et al. due to their seemingly contradictory results (Vishvanath et al., 2017). Vishvanath and colleagues wondered if the apparent discrepancies between our results could stem from the fact we used a HFD in which 42% of kilocalories are drawn from milkfat instead of the more frequently used lard-based HFD (60% of kilocalories drawn from fat) (Vishvanath et al., 2017). In the present study, we have employed the well-established lard-based HFD, achieving results similar to those we previously reported with the less caloric HFD (that is, lack of significant adipocyte labeling by the mural-cell-specific *Tbx18-CreERT2*). However, our histological analyses have also provided an explanation for the discrepancy of results between our teams. Vishvanath et al. lineage traced APs using a *Pdgfrb*-inducible Cre, reasoning that PDGFRβ expression is mural cell specific (Vishvanath et al., 2016). Here, we showed that in adipose depots, PDGFRβ is expressed by both mural cells (pericytes and vascular smooth muscle cells) and fibroblasts (adventitial and capsular). As such, labeling of *de novo* adipocytes observed by Vishvanath and colleagues is likely a result of fibroblast progenitors being labeled by the *Pdgfrb*-inducible Cre, similar to *de novo* adipocyte labeling observed here using *Pdgfra-MerCreMer*. Importantly, our histological results are in agreement with recent single-cell RNA sequencing (RNA-seq) studies suggesting that adipogenic progenitors express both PDGFRα and PDGFRβ (Burl et al., 2018). Quantitatively, using their *Pdgfrb*-inducible Cre (transgenic allele, with expression controlled by a large fragment of the *Pdgfrb* promoter), Vishvanath et al. observed 10% adipocyte labeling in pgWAT in HFD-fed animals (Vishvanath et al., 2016), whereas using a *Pdgfra-CreERT2* plasmid artificial chromosome (PAC) transgenic allele (Rivers et al., 2008) distinct from the knockin *Pdgfra-MerCreMer* we used, Lee and colleagues reported 15% adipocyte labeling in pgWAT in HFD animals (Lee et al., 2012). Our results with the *Pdgfra-MerCreMer* were somewhat higher (32.18% adipocyte labeling in pgWAT of HFD-fed animals), a fact that might be explained either by different

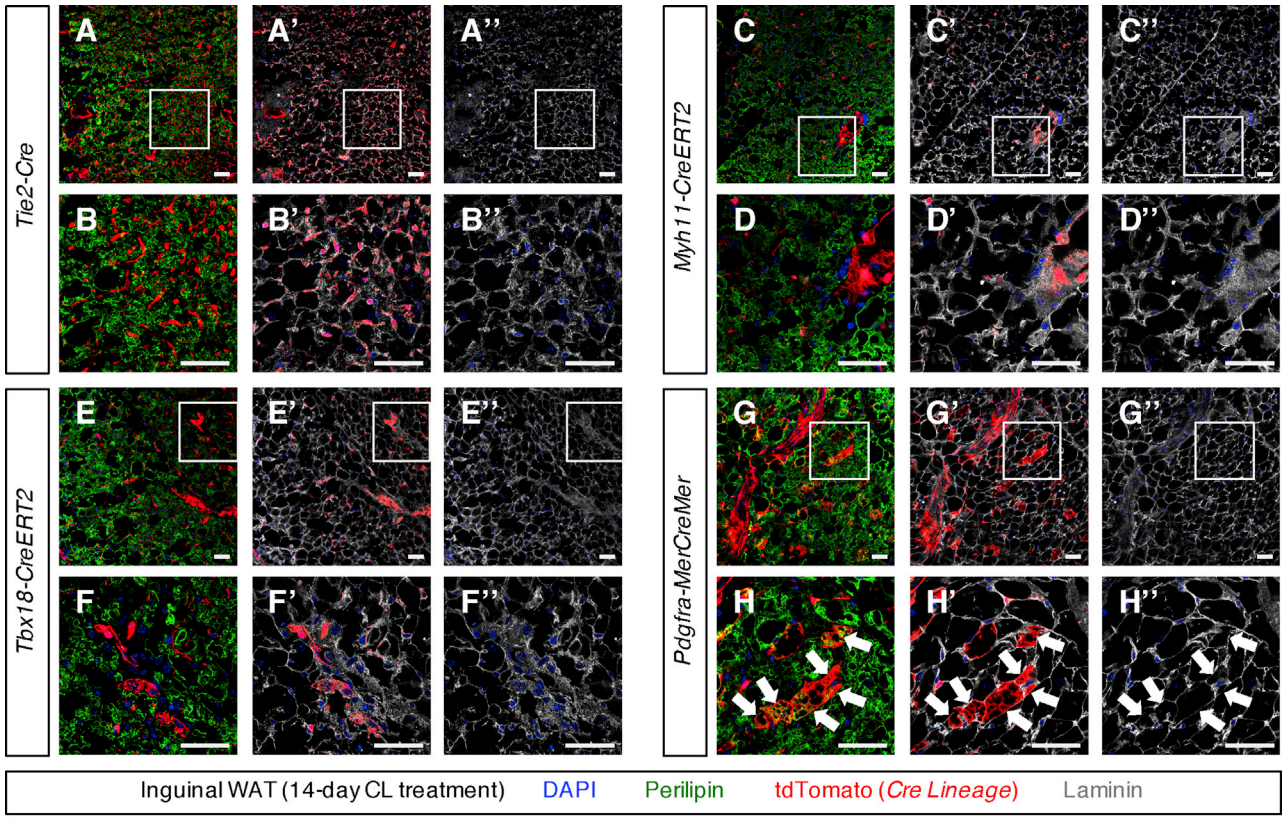

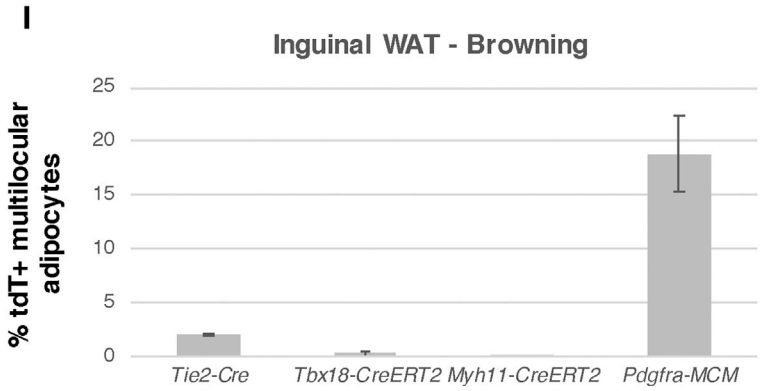

Figure 4. PDGFRα$^+$ Fibroblasts Were the Only Vascular Cell Type Significantly Contributing to Beiging of Inguinal WAT

(A and B) After 14 days of CL treatment, *Tie2-Cre*-labeled endothelial cells did not acquire a multilocular adipocyte fate.

(C–F) Mural cells labeled by *Myh11-CreERT2* (C and D) or *Tbx18CreERT2* (E and F) did not significantly transdifferentiate to beige adipocytes after 14 days of CL treatment.

(G and H) After 14 days of CL treatment, it was possible to detect multiple multilocular adipocytes lineage traced by *Pdgfra-MerCreMer*, indicating these cells were derived from PDGFRα-expressing progenitors by *de novo* adipogenesis.

(I) Quantification of rates of beige adipocyte labeling by Cres specifically hitting distinct cell types of the vascular wall. Data are represented as mean ± SEM (n = 3 per experimental group).

(B), (D), (F), and (H) represent higher magnifications of areas boxed in (A), (C), (E), and (G), respectively. Bars represent 50 μm in all panels.

See also Figure S4.

efficiencies of labeling of PDGFRα cells by distinct Cres or by mouse-strain-specific properties (our studies were conducted in outbred Black-Swiss animals, which typically have larger body weights than inbred mice). Importantly, the *Pdgfra-MerCreMer* allele we used was produced by knocking in the inducible Cre cassette into the *Pdgfra* locus, disrupting the

endogenous transcript (Ding et al., 2013). PDGFRα signaling is known to negatively regulate *de novo* adipogenesis (Sun et al., 2017), so it is possible that *Pdgfra* heterozygosity might have resulted in an increase in *de novo* adipogenesis. However, our immunostaining results (Figures 3I–3L) showing high levels of PDGFRα protein in fibroblasts of *Pdgfra-MerCreMer* tissues argue against this potentially confounding factor. Our strategy for lineage tracing mural cells or fibroblasts was based on tamoxifen administration to promote the activity of inducible Cres. A recent report suggested tamoxifen administration can promote adipocyte death and weight loss followed by a compensatory wave of *de novo* adipogenesis (Ye et al., 2015). This phenomenon could also contribute to the high rates of adipocyte labeling we observed in *Pdgfra-MerCreMer* lineage-traced animals. However, this is not likely to have influenced our quantitative analyses, as animals included in our studies displayed increased body weight 1 week post-tamoxifen (Figure S2A) and, unlike observations reported by Ye et al., our results did not reveal any evidence of lipolysis or adipocyte death at early time points post-induction (Figures 2, 3, and S2). Taking into consideration these potentially confounding factors, it will be of interest if other *Pdgfra*- and tamoxifen-independent tools are generated to label adipose tissue fibroblasts and quantify their contribution to *de novo* adipogenesis.

Our quantitative results are highly compatible with findings reported by Jeffery and colleagues, who, using an adiponectin-CreER to label adipocytes, observed that in visceral WAT, after 8 weeks of HFD, ~25% of adipocytes had been formed by *de novo* adipogenesis from APs (Jeffery et al., 2015). Experiments using the AdipoChaser in white adipose depots only detected *de novo* adipogenesis after long periods of HFD (Wang et al., 2013), whereas we could detect early multilocular adipocytes as early as 5 days post-conclusion of tamoxifen induction (8 days post-initiation of induction). These differences in timing are likely a consequence of the two distinct systems used; the AdipoChaser is optimized to visualize mature adipocytes, whereas our system labels progenitors rather than mature cells, thus allowing visualization of all steps from fibroblastic APs to mature adipocytes. Importantly, the fluorescent indicator tdTomato is excluded from lipid vesicles, allowing for ready visualization of otherwise less evident, small, multilocular adipocytes. This property of our models for lineage tracing allowed us to observe that the early steps of fibroblast-to-white adipocyte conversion involve an intermediate beige adipocyte phenotype. Of note, classification of these cells as beige adipocytes was entirely based on morphological criteria (multilocular adipocytes of smaller dimensions nestled between mature white adipocytes) (Figures 3I–3L), because in non-stimulated animals, beige adipocytes have low basal expression of UCP1 and reduced respiratory activity (Wu et al., 2012). At the time point our pulse-chase studies were initiated (8-week-old animals), the majority of white adipocytes in mouse have already developed. As such, our analyses do not provide information as to whether this multilocular intermediate phenotype is a developmental feature shared by all white adipocytes or if it is specific to adult *de novo* white adipogenesis from fibroblastic progenitors. To clarify this open question and assess the effect of age on rates of *de novo* adipogenesis, it will be of future interest to complement results here reported with additional lineage-tracing studies performed on earlier and later developmental time points.

We also provide evidence for *de novo* adipogenesis from capsular PDGFRα$^+$ fibroblasts in pgWAT, which is consistent with a previous suggestion that mesothelial cells might act as a potential source of new adipocytes (Chau et al., 2014). The properties and embryonic origin of the capsular fibroblasts surrounding white adipose depots can be quite distinct. Capsular fibroblasts of coelomic WAT have a mesothelial origin and are tightly compacted, forming a thin, highly cellular dense protective layer (Figures 3A and 3B). In subcutaneous WAT, these cells likely share a similar origin with dermal reticular fibroblasts (Driskell and Watt, 2015) and form a less compact structure that is richer in extracellular matrix (Figures 3C and 3D) and has a gelatinous nature upon dissection. 8 weeks after induction, we observed, immediately adjacent to the external capsule of pgWAT, foci of extensive labeling of adipocytes by *Pdgfra-MerCreMer* (Figures 3E and 3F), suggesting a major contribution to *de novo* adipogenesis from lineage-traced capsular fibroblasts. This contribution was observed both in chow or HFD. In ingWAT, adipocyte labeling adjacent to capsular fibroblasts was also observed, but the pattern of labeling was less extensive relative to that seen for pericapsular labeling in pgWAT (Figures 3G and 3H), suggesting that capsular fibroblasts provide a smaller contribution to the adipocyte pool in iWAT relative to pgWAT.

A limitation of our studies is that the lineage-tracing strategies employed do not allow us to discriminate whether all adipose tissue fibroblasts have similar adipogenic potential or if a subset of these cells have preferential adipogenic properties. Similarly, our results do not allow us to conclude whether subpopulations of PDGFRα$^+$ cells give rise to brown, beige, and white adipocytes separately or if there is a common progenitor for all adipocyte types. To clarify these open questions, it will be of future interest to perform clonal lineage tracing studies using the *Pdgfra-MerCreMer* allele.

Our beiging experiments in ingWAT induced by β3-adrenergic stimulation (Figure 4) produced results that harmonize previous studies, showing that beiging received a significant contribution (~20% of all beige adipocytes) of *de novo* adipogenesis from fibroblastic APs that were positive for not only PDGFRα (Lee et al., 2012) but also PDGFRβ (Vishvanath et al., 2016). Remaining beige adipocytes were not lineage traced, indicating they were derived from preexisting adipocytes. These estimates are highly consistent with previous studies reporting that ~75% of all CL-induced beige adipocytes are derived from preexisting adipocytes labeled by adiponectin-CreERT2 (Jiang et al., 2017). Our experiments with *Myh11-CreERT2* demonstrated this Cre labeled not only vascular smooth muscle but also pericytes, a surprising observation considering that at the protein level, pericytes did not express markers of mature vascular smooth muscle (Figure S4). Our analyses of beiging of ingWAT did not support previous findings of conversion of vascular smooth muscle into beige adipocytes, despite being performed with the same *Myh11-CreERT2* allele (Long et al., 2014). Our results with *Tbx18-CreERT2*, which, like *Myh11-CreERT2*, specifically labels vascular smooth muscle and pericytes

(Guimaraes-Camboa et al., 2017), also demonstrated lack of contribution of vascular mural cells to *de novo* beiging. The apparent discrepancy between results of Long et al. and our results may reside in the use of distinct experimental beiging models: Long et al. induced beiging by exposing animals to cold, whereas we employed a model based on β3-adrenergic stimulation. Consistent with this idea, Jiang and colleagues have recently proposed these two models rely on distinct cellular mechanisms, with smooth muscle origin of beige adipocytes being exclusively detected in the protocol induced by cold (Jiang et al., 2017). Considering that beiging of WAT is a potential strategy to fight obesity (Giordano et al., 2016; Lee et al., 2014), it will be important for additional groups to clearly test the impact of distinct genetic and environmental variables in the cellular and physiological outcomes of beiging stimuli.

In conclusion, results reported here provide a significant contribution toward the harmonization of a controversial field, suggesting that *in vivo* APs are fibroblasts (perivascular or capsular) expressing both PDGFRα and PDGFRβ. PDGFRα$^+$, PDGFRβ$^+$ APs significantly contributed to white, brown, and beige adipocytes in the distinct models tested. Our analyses also suggest that conversion of fibroblast APs to mature white adipocytes involves an intermediate beige phenotype. This finding, together with the notion that a major process in beiging of white depots is the reversal of mature white adipocytes to a multilocular beige state, supports the idea that white and beige adipocyte phenotypes might correspond to distinct states of a single cell type rather than distinct cellular identities.

STAR★METHODS

Detailed methods are provided in the online version of this paper and include the following:

- KEY RESOURCES TABLE
- LEAD CONTACT AND MATERIALS AVAILABILITY
- EXPERIMENTAL MODEL AND SUBJECT DETAILS
  - Animals
- METHOD DETAILS
  - Experimental Design
  - Tamoxifen Induction
  - Fluorescent immunohistochemistry/immunocytochemistry
- QUANTIFICATION AND STATISTICAL ANALYSIS
- DATA AND CODE AVAILABILITY

SUPPLEMENTAL INFORMATION

Supplemental Information can be found online at https://doi.org/10.1016/j.celrep.2019.12.046.

ACKNOWLEDGMENTS

This work was supported by grants from the German Center for Cardiovascular Research (DZHK, Junior Research Group) and Excellence Cluster Cardiopulmonary Institute to N.G.-C., as well as a Leducq transatlantic network grant to S.M.E. and National Institutes of Health (NIH) grants to J.C. and S.M.E. J.C. is the American Heart Association Endowed Chair in Cardiovascular Research.

AUTHOR CONTRIBUTIONS

Conceptualization, Methodology, and Funding Acquisition, S.M.E. and N.G.-C.; Investigation, P.C., D.M., S.S., L.Z., V.L., and N.G.-C.; Formal Analysis and Data Curation, D.M. and N.G.-C.; Resources, W.B.S., H.K., J.C., and S.D.; Supervision, S.D.; Writing—Original Draft, P.C., S.M.E., and N.G.-C.; Writing—Review and Editing: D.M., S.S., V.L., and S.D.

DECLARATION OF INTERESTS

The authors declare no competing interests.

Received: September 9, 2019
Revised: October 30, 2019
Accepted: December 13, 2019
Published: January 14, 2020

REFERENCES

Andrae, J., Gallini, R., and Betsholtz, C. (2008). Role of platelet-derived growth factors in physiology and medicine. Genes Dev. *22*, 1276–1312.

Armulik, A., Genové, G., and Betsholtz, C. (2011). Pericytes: developmental, physiological, and pathological perspectives, problems, and promises. Dev. Cell *21*, 193–215.

Barbatelli, G., Murano, I., Madsen, L., Hao, Q., Jimenez, M., Kristiansen, K., Giacobino, J.P., De Matteis, R., and Cinti, S. (2010). The emergence of cold-induced brown adipocytes in mouse white fat depots is determined predominantly by white to brown adipocyte transdifferentiation. Am. J. Physiol. Endocrinol. Metab. *298*, E1244–E1253.

Berry, R., and Rodeheffer, M.S. (2013). Characterization of the adipocyte cellular lineage in vivo. Nat. Cell Biol. *15*, 302–308.

Blanchette-Mackie, E.J., Dwyer, N.K., Barber, T., Coxey, R.A., Takeda, T., Rondinone, C.M., Theodorakis, J.L., Greenberg, A.S., and Londos, C. (1995). Perilipin is located on the surface layer of intracellular lipid droplets in adipocytes. J. Lipid Res. *36*, 1211–1226.

Burl, R.B., Ramseyer, V.D., Rondini, E.A., Pique-Regi, R., Lee, Y.H., and Granneman, J.G. (2018). Deconstructing adipogenesis induced by beta3-adrenergic receptor activation with single-cell expression profiling. Cell Metab. *28*, 300–309.

Cai, C.L., Martin, J.C., Sun, Y., Cui, L., Wang, L., Ouyang, K., Yang, L., Bu, L., Liang, X., Zhang, X., et al. (2008). A myocardial lineage derives from Tbx18 epicardial cells. Nature *454*, 104–108.

Chau, Y.Y., Bandiera, R., Serrels, A., Martínez-Estrada, O.M., Qing, W., Lee, M., Slight, J., Thornburn, A., Berry, R., McHaffie, S., et al. (2014). Visceral and subcutaneous fat have different origins and evidence supports a mesothelial source. Nat. Cell Biol. *16*, 367–375.

Clark, E.R., and Clark, E.L. (1940). Microscopic studies of the new formation of fat in living adult rabbits. Am. J. Anat. *67*, 255–285.

Crossno, J.T., Jr., Majka, S.M., Grazia, T., Gill, R.G., and Klemm, D.J. (2006). Rosiglitazone promotes development of a novel adipocyte population from bone marrow-derived circulating progenitor cells. J. Clin. Invest. *116*, 3220–3228.

Ding, G., Tanaka, Y., Hayashi, M., Nishikawa, S., and Kataoka, H. (2013). PDGF receptor alpha+ mesoderm contributes to endothelial and hematopoietic cells in mice. Dev. Dyn. *242*, 254–268.

Driskell, R.R., and Watt, F.M. (2015). Understanding fibroblast heterogeneity in the skin. Trends Cell Biol. *25*, 92–99.

Gesta, S., Tseng, Y.H., and Kahn, C.R. (2007). Developmental origin of fat: tracking obesity to its source. Cell *131*, 242–256.

Giordano, A., Frontini, A., and Cinti, S. (2016). Convertible visceral fat as a therapeutic target to curb obesity. Nat. Rev. Drug Discov. *15*, 405–424.

Granneman, J.G., Li, P., Zhu, Z., and Lu, Y. (2005). Metabolic and cellular plasticity in white adipose tissue I: effects of beta3-adrenergic receptor activation. Am. J. Physiol. Endocrinol. Metab. *289*, E608–E616.

Guimaraes-Camboa, N., Cattaneo, P., Sun, Y., Moore-Morris, T., Gu, Y., Dalton, N.D., Rockenstein, E., Masliah, E., Peterson, K.L., Stallcup, W.B., et al. (2017). Pericytes of multiple organs do not behave as mesenchymal stem cells in vivo. Cell Stem Cell *20*, 345–359.

Himms-Hagen, J., Melnyk, A., Zingaretti, M.C., Ceresi, E., Barbatelli, G., and Cinti, S. (2000). Multilocular fat cells in WAT of CL-316243-treated rats derive directly from white adipocytes. Am. J. Physiol. Cell Physiol. *279*, C670–C681.

Jeffery, E., Church, C.D., Holtrup, B., Colman, L., and Rodeheffer, M.S. (2015). Rapid depot-specific activation of adipocyte precursor cells at the onset of obesity. Nat. Cell Biol. *17*, 376–385.

Jiang, Y., Berry, D.C., and Graff, J.M. (2017). Distinct cellular and molecular mechanisms for β3 adrenergic receptor-induced beige adipocyte formation. eLife *6*, e30329.

Kisanuki, Y.Y., Hammer, R.E., Miyazaki, J., Williams, S.C., Richardson, J.A., and Yanagisawa, M. (2001). Tie2-Cre transgenic mice: a new model for endothelial cell-lineage analysis in vivo. Dev. Biol. *230*, 230–242.

Koh, Y.J., Kang, S., Lee, H.J., Choi, T.S., Lee, H.S., Cho, C.H., and Koh, G.Y. (2007). Bone marrow-derived circulating progenitor cells fail to transdifferentiate into adipocytes in adult adipose tissues in mice. J. Clin. Invest. *117*, 3684–3695.

Lee, Y.H., Petkova, A.P., Mottillo, E.P., and Granneman, J.G. (2012). In vivo identification of bipotential adipocyte progenitors recruited by β3-adrenoceptor activation and high-fat feeding. Cell Metab. *15*, 480–491.

Lee, Y.H., Mottillo, E.P., and Granneman, J.G. (2014). Adipose tissue plasticity from WAT to BAT and in between. Biochim. Biophys. Acta *1842*, 358–369.

Long, J.Z., Svensson, K.J., Tsai, L., Zeng, X., Roh, H.C., Kong, X., Rao, R.R., Lou, J., Lokurkar, I., Baur, W., et al. (2014). A smooth muscle-like origin for beige adipocytes. Cell Metab. *19*, 810–820.

Madisen, L., Zwingman, T.A., Sunkin, S.M., Oh, S.W., Zariwala, H.A., Gu, H., Ng, L.L., Palmiter, R.D., Hawrylycz, M.J., Jones, A.R., et al. (2010). A robust and high-throughput Cre reporting and characterization system for the whole mouse brain. Nat. Neurosci. *13*, 133–140.

Majka, S.M., Fox, K.E., Psilas, J.C., Helm, K.M., Childs, C.R., Acosta, A.S., Janssen, R.C., Friedman, J.E., Woessner, B.T., Shade, T.R., et al. (2010). De novo generation of white adipocytes from the myeloid lineage via mesenchymal intermediates is age, adipose depot, and gender specific. Proc. Natl. Acad. Sci. USA *107*, 14781–14786.

Nagase, I., Yoshida, T., Kumamoto, K., Umekawa, T., Sakane, N., Nikami, H., Kawada, T., and Saito, M. (1996). Expression of uncoupling protein in skeletal muscle and white fat of obese mice treated with thermogenic beta 3-adrenergic agonist. J. Clin. Invest. *97*, 2898–2904.

Rivers, L.E., Young, K.M., Rizzi, M., Jamen, F., Psachoulia, K., Wade, A., Kessaris, N., and Richardson, W.D. (2008). PDGFRA/NG2 glia generate myelinating oligodendrocytes and piriform projection neurons in adult mice. Nat. Neurosci. *11*, 1392–1401.

Rutkowski, J.M., Stern, J.H., and Scherer, P.E. (2015). The cell biology of fat expansion. J. Cell Biol. *208*, 501–512.

Sera, Y., LaRue, A.C., Moussa, O., Mehrotra, M., Duncan, J.D., Williams, C.R., Nishimoto, E., Schulte, B.A., Watson, P.M., Watson, D.K., et al. (2009). Hematopoietic stem cell origin of adipocytes. Exp. Hematol. *37*, 1108–1120.

Sun, C., Berry, W.L., and Olson, L.E. (2017). PDGFRα controls the balance of stromal and adipogenic cells during adipose tissue organogenesis. Development *144*, 83–94.

Tang, W., Zeve, D., Suh, J.M., Bosnakovski, D., Kyba, M., Hammer, R.E., Tallquist, M.D., and Graff, J.M. (2008). White fat progenitor cells reside in the adipose vasculature. Science *322*, 583–586.

Tran, K.V., Gealekman, O., Frontini, A., Zingaretti, M.C., Morroni, M., Giordano, A., Smorlesi, A., Perugini, J., De Matteis, R., Sbarbati, A., et al. (2012). The vascular endothelium of the adipose tissue gives rise to both white and brown fat cells. Cell Metab. *15*, 222–229.

Vishvanath, L., MacPherson, K.A., Hepler, C., Wang, Q.A., Shao, M., Spurgin, S.B., Wang, M.Y., Kusminski, C.M., Morley, T.S., and Gupta, R.K. (2016). Pdgfrβ+ mural preadipocytes contribute to adipocyte hyperplasia induced by high-fat-diet feeding and prolonged cold exposure in adult mice. Cell Metab. *23*, 350–359.

Vishvanath, L., Long, J.Z., Spiegelman, B.M., and Gupta, R.K. (2017). Do adipocytes emerge from mural progenitors? Cell Stem Cell *20*, 585–586.

Wang, Q.A., Tao, C., Gupta, R.K., and Scherer, P.E. (2013). Tracking adipogenesis during white adipose tissue development, expansion and regeneration. Nat. Med. *19*, 1338–1344.

Wirth, A., Benyó, Z., Lukasova, M., Leutgeb, B., Wettschureck, N., Gorbey, S., Orsy, P., Horváth, B., Maser-Gluth, C., Greiner, E., et al. (2008). G12-G13-LARG-mediated signaling in vascular smooth muscle is required for salt-induced hypertension. Nat. Med. *14*, 64–68.

Wu, J., Boström, P., Sparks, L.M., Ye, L., Choi, J.H., Giang, A.H., Khandekar, M., Virtanen, K.A., Nuutila, P., Schaart, G., et al. (2012). Beige adipocytes are a distinct type of thermogenic fat cell in mouse and human. Cell *150*, 366–376.

Ye, R., Wang, Q.A., Tao, C., Vishvanath, L., Shao, M., McDonald, J.G., Gupta, R.K., and Scherer, P.E. (2015). Impact of tamoxifen on adipocyte lineage tracing: Inducer of adipogenesis and prolonged nuclear translocation of Cre recombinase. Mol. Metab. *4*, 771–778.

Young, P., Arch, J.R., and Ashwell, M. (1984). Brown adipose tissue in the parametrial fat pad of the mouse. FEBS Lett. *167*, 10–14.

STAR★METHODS

KEY RESOURCES TABLE

REAGENT or RESOURCE	SOURCE	IDENTIFIER
Antibodies		
Rat monoclonal anti-CD31/PECAM (clone MEC13.3)	BD PharMingen	Cat#: 550274; RRID: AB_393571
Rabbit monoclonal (EPR3864) anti-ERG	Abcam	Cat#: ab92513; RRID: AB_2630401
Chicken polyclonal anti-Laminin	Abcam	Cat#: ab14055; RRID: AB_300883
Goat polyclonal anti-PDGFRα	R&D Systems	Cat#: AF1062; RRID: AB_2236897
Rabbit polyclonal anti-PDGFRβ	Laboratory of William Stallcup	RRID: AB_2783647
Rabbit monoclonal (D1D8) anti-Perilipin	Cell Signaling Technology	Cat#: 9349; RRID: AB_2167270
Goat polyclonal anti-Perilipin	Abcam	Cat#: ab61682; RRID: AB_10829911
Rabbit polyclonal anti-Smooth muscle α-actin	Abcam	Cat#: ab5694; RRID: AB_2223021
Chemicals, Peptides, and Recombinant Proteins		
DAPI (4',6-Diamidino-2-Phenylindole, Dihydrochloride)	Life Technologies	Cat#: D1306
Donkey Serum	Merck Millipore	Cat#: S30-100mL
Paraformaldehyde, 16% aqueous solution	Electron Microscopy Sciences	Cat#: 15710
Tamoxifen	Sigma-Aldrich	Cat#: T5648
Teklad LM-485 Rodent Diet, Irradiated	Envigo	Cat#: 7912
High Fat Diet: Rodent Diet With 60 kcal% Fat	Research diets Inc.	Cat#: D12492
Experimental Models: Organisms/Strains		
Mouse: Black Swiss (outbred wild-type mice): NIHBL(S)	Charles River	Strain code: 492
Mouse: *Myh11*-CreERT2: *Tg(Myh11-cre/ERT2)*^{1Soff}	Wirth et al., 2008	MGI#: 3819270; JAX#: 019079
Mouse: *Pdgfra-MerCreMer: Pdgfra*$^{tm1.1(cre/Esr1*)Nshk}$	Ding et al., 2013	MGI#: 5475226; JAX#: N/A
Mouse: *Rosa26-tdTomato* (Ai9): *Gt(ROSA) 26Sor*$^{tm14(CAG-tdTomato)Hze}$	Madisen et al., 2010	MGI#: 3809523; JAX stock#: 007905
Mouse: *Tbx18-H2B:GFP: Tbx18*$^{tm1.1Sev}$	Cai et al., 2008	MGI#: 5529155; JAX#: 031519
Mouse: *Tbx18*-CreERT2: *Tbx18*$^{tm3.1(cre/ERT2)Sev}$	Guimaraes-Camboa et al., 2017	MGI#: 6113477; JAX#: 031520
Mouse: *Tie2*-Cre: *Tg(Tek-cre)*^{1Ywa}	Kisanuki et al., 2001	MGI#: 2450311; JAX stock#: 008863
Software and Algorithms		
Leica Application Suite LAS-X	Leica	https://www.leica-microsystems.com/products/microscope-software/p/leica-las-x-ls/
Volocity®	PerkinElmer	https://www.perkinelmer.com/lab-products-and-services/resources/whats-new-volocity-6-3.html

LEAD CONTACT AND MATERIALS AVAILABILITY

Further information and requests for resources and reagents should be directed to and will be fulfilled by the Lead Contact, Nuno Guimarães-Camboa (ncamboa@med.uni-frankfurt.de). This study did not generate new unique reagents.

EXPERIMENTAL MODEL AND SUBJECT DETAILS

Animals

Lineage tracing experiments were conducted using male laboratory mice (*Mus musculus*) kept on an outbred background (Black-Swiss, Charles River laboratories). All care of transgenic mouse models was in compliance with the Guide for the Care and Use of Laboratory Animals published by the US National Institutes of Health, as well as institutional guidelines at the University of California, San Diego. Mice were housed in plastic cages with filtered air intake ports and automatic water dispensers (Tecniplast) on a 12-hour light cycle. Animals were maintained in a specific-pathogen-free vivarium and were not involved in any experimental procedures or exposed to any pharmaceutical agents prior to the beginning of our time course analyses. *Tie2-Cre*, expressing Cre recombinase under the control of the *Tie2* promotor/enhancer (Kisanuki et al., 2001) was a king gift from Masashi Yanagisawa.

The *Tbx18-H2B:GFP* transcriptional indicator was generated in our laboratory and has been previously shown to faithfully recapitulate the patterns of *Tbx18* expression (Cai et al., 2008). *The Tbx18-CreERT2* allele was generated in our laboratory and has been previously shown to be highly efficiently in the labeling of pericytes and vascular smooth muscle of different adipose depots (Guimaraes-Camboa et al., 2017). The *Pdgfra-MerCreMer* knock-in allele (http://www2.clst.riken.jp/arg/mutant%20mice%20list.html – accession number CDB0674K) was kindly provided by Hiroshi Kataoka (Ding et al., 2013). The *Rosa26-tdTomato* reporter allele generated by Hongkui Zeng (Madisen et al., 2010) and *Myh11-CreERT2* generated by Stefan Offermanns (Wirth et al., 2008) were obtained from the JAX laboratories (stock numbers: 007905 and 019079, respectively).

METHOD DETAILS

Experimental Design

Male mice were fed irradiated chow (Teklad LM-485, Harlan Laboratories, catalog number 7912) until 8 weeks of age. 8-week-old mice were induced with tamoxifen and, depending on the experimental group, maintained on chow or transferred to HFD (60% kcal fat, Research diets Inc., D12492). The body weight of each animal included in our studies was assessed at end of the tamoxifen pulse and, subsequently, every 7 days during the chase period. After 8 weeks of chow or HFD, the body weight at the experimental term was determined and animals were euthanized, with the aorta and all major fat depots being processed for histological analyses. For each Cre, cages of lineage traced animals were randomly allocated to one of the experimental groups (chow or HFD) by flipping a coin. To ensure blinded results, tissue collection and imaging/quantification tasks were performed by different researchers. The researcher responsible for imaging and quantification of adipocyte labeling was not aware of the experimental group (chow or HFD) each animal belonged to. Prior to analyses of fat depots, aortae of animals from all groups were processed for fluorescent microscopy to ensure efficient labeling of the target cellular population. Animals with reduced labeling of target cell types (indicating inefficient tamoxifen induction) or presenting generalized labeling, rather than cell-type-specific labeling (an indication of Cre leakiness), were excluded from our studies.

Tamoxifen Induction

Induction of recombinase activity was achieved by intra-peritoneal injection of 250 μL of a 10 mg/mL tamoxifen solution in three consecutive days, starting at 8 weeks of age. Tamoxifen was purchased from Sigma (catalog number T5648), dissolved in 10 mL of 100% ethanol and subsequently diluted in 90 mL of sesame oil (Sigma, catalog number S3547). Aliquots were stored at −20°C for a maximum of 6 months.

Fluorescent immunohistochemistry/immunocytochemistry

Dissected fat pads were fixed overnight in 4% paraformaldehyde (Electron Microscope Sciences) at 4°C, dehydrated in a sucrose gradient and frozen in O.C.T. compound (Tissue-Tek). Histological sections (50 μm thick for white adipose depots and 10 μm thick for aortae and brown adipose depots) were prepared from frozen blocks using a Leica CM3050S cryostat. Tissue sections were permeabilized in PBS-0.5% Triton for 20 min and incubated for one h at room temperature in blocking solution (PBS-0.1% Triton, 10% donkey serum, 5% skim milk) prior to overnight primary antibody incubation (4°C, in blocking solution). A list of all primary antibodies used, their providers, and their dilutions can be found in the Key Resources Table. AlexaFluor(488;555;647)-conjugated secondary antibodies raised in donkey (Life Technologies), diluted 1:400 in blocking solution, were used for detection of primary antibodies (incubation time = 75 min, at room temperature). DAPI (Life Technologies) was used for labeling of nuclei. Image acquisition was performed using a Leica SP8 confocal microscope and image editing done using Volocity (PerkinElmer). Images were acquired as Z stacks of 10 to 16 plans with 0.5 μm spacing between consecutive plans and are displayed as maximum intensity projections.

QUANTIFICATION AND STATISTICAL ANALYSIS

All labeling quantifications were performed in at least 3 animals, with a minimal of 5 distinct sections being imaged and counted per animal. In all graphs, data are presented as the mean ± standard error of the mean. In Figure legends, n = represents number of animals. For each Cre and adipose depot, differences in rates of adipocyte labeling between chow and HFD groups were probed for statistical significance using unpaired, 2-tailed Student's t test.

DATA AND CODE AVAILABILITY

The confocal microscopy datasets supporting the current study have not been deposited in a public repository (due to the large number of files involved), but are available from the lead author on request.